JOURNAL OF MATERIALS SCIENCE 23 (1988) 337–342

Decomposition behaviours of dopant-free and doped solid solutions in the TiO_2–SnO_2 system

J. TAKAHASHI, M. KUWAYAMA*, H. KAMIYA, M. TAKATSU
Department of Materials Science and Engineering, Nagoya Institute of Technology, Nagoya 466, Japan

T. OOTA, I. YAMAI
Ceramic Engineering Research Laboratory, Nagoya Institute of Technology, Tajimi 507, Japan

Decomposition behaviours, including phase separation by the spinodal mechanism, were investigated for selected compositions of $x = 0.7$, 0.5 and 0.3 in $Ti_xSn_{1-x}O_2$ alloy. Inside the coherent spinodal, an equimolar alloy was found to decompose most rapidly at 1100° C and the decomposition rate decreased as the annealing temperature increased. The difference in the rate of decomposition outside the spinodal between $x = 0.7$ and $x = 0.3$ alloys suggested that the ionic mobility of diffusing tin was much slower than that of titanium in the alloy system. The effect of some dopants on the decomposition rate was also examined. Doping with tungsten or antimony atoms strongly suppressed the phase separation both inside and outside the spinodal, especially resulting in a prolonged stabilization of $x = 0.7$ alloy. The role of the dopants in affecting the decomposition rate is discussed in relation to selective substitution of the doping atoms in the tin or titanium sublattice.

1. Introduction

The tetragonal TiO_2–SnO_2 solid-solution system contains a subsolidus immiscibility gap [1], inside which phase separation is characterized by coherent spinodal decomposition corresponding to [0 0 1] modulations. Phase separation by the spinodal mechanism which was theoretically interpreted by Cahn [2, 3] has been experimentally observed in a number of metallic binary systems. In particular, the development of superior magnetic materials such as Alnico alloys and the toughening of various metallic alloys are closely associated with spinodal decomposition. In crystalline oxide systems, the TiO_2–SnO_2 solid solutions have been shown to decompose spinodally by Stubican and Schultz [4, 5]. Since their first work on spinodal decomposition, a number of theoretical and some experimental studies have been conducted for the TiO_2–SnO_2 system. Park *et al.* [6] concisely reviewed the phase separation of the system in their study on the initial process of spinodal decomposition.

Recently, materials research on a number of titanates and stannates has been performed for practical application to electric devices. Alternative substitution of titanium by tin and/or tin by titanium and further cation substitution with foreign atoms have been occasionally attempted to give a variety of electric properties for the materials. However, in spite of extensive basic investigations and the practical development of oxide systems containing both titanium and tin atoms, the fundamental behaviour of the cation diffusion or substitutional incorporation of foreign atoms in the systems is not fully understood yet. Especially for the original TiO_2–SnO_2 system, no information concerning the diffusivities of titanium and tin in solid solutions is available. In addition, a few experimental studies on doping effect are reported on the phase separation of the same system [7, 8]. In the present paper, therefore, to obtain some information about cation diffusion and substitution, we examined the decomposition behaviours of some selected dopant-free and doped oxide alloys inside and outside the spinodal in the TiO_2–SnO_2 system.

2. Experimental procedures

Powder samples of crystalline solutions, whose compositions were mostly $x = 0.7$, 0.5 and 0.3 in $Ti_xSn_{1-x}O_2$ (hereafter referred to as T_7S_3, T_5S_5 and T_3S_7, respectively), were prepared from highly pure TiO_2 and SnO_2. For T_7S_3 and T_3S_7 oxide alloys, mixed powders with known ratios of the corresponding oxides were heated at 1500° C for 12 h in alumina crucibles. They were then allowed to cool rapidly and were pulverized by wet-grinding for successive heating. This heating operation was repeated to minimize the compositional heterogeneity of the alloy produced by solid-state reaction. An equimolar T_5S_5 alloy was heat-treated by three runs of the cyclic heating procedure described above as a first heating operation. Then T_5S_5 powder was finally synthesized by further heating of a pressed compact of the preheated sample at 1500° C for 6 h and by immediate quenching into water.

Phase separation was studied for oxide alloys with selected compositions by annealing at 1000 to 1300° C for various duration up to 100 h. (Sample compositions

* *Present address:* Kawasaki Steel K.K., Japan.

0022–2461/88 $03.00 + .12

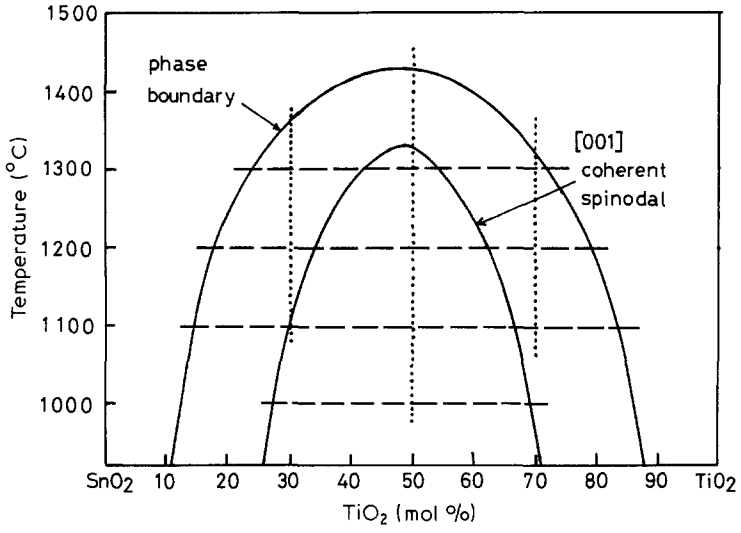

Figure 1 Phase diagram of the TiO_2–SnO_2 system determined by Park *et al.* [1]. Broken and dotted lines denote annealing temperature and composition of alloys examined in this work, respectively.

and annealing temperatures examined in the present work are shown in the phase diagram of Fig. 1.) Relative intensity changes in the X-ray diffraction profile of the titanium-rich or tin-rich phase produced with the promotion of phase separation was measured by conventional X-ray diffractometry (XRD). Changes in lattice parameters of alloys with phase separation were concurrently estimated using purified copper (5 N) as an internal standard.

Fourteen oxides were first selected as dopants; ZrO_2, V_2O_5, Nb_2O_5, Ta_2O_5, MoO_2, WO_3, MnO_2, CoO, NiO, CuO, In_2O_3, PbO, Sb_2O_3 and Bi_2O_3. T_7S_3 alloy to which these oxides had been added at 5 or 10 mol % was heated at 1400° C for 5 h and then annealed at 1100° C for 5 h. XRD results indicated that phase separation by a nucleation and growth mechanism was suppressed for alloys with the addition of ZrO_2, Ta_2O_5, WO_3 and Sb_2O_3. Therefore to examine the effect of these dopants on the phase separation including spinodal decomposition, TiO_2–SnO_2 alloys containing the separate dopant were fabricated and annealed. The annealing temperatures employed in decomposition experiments on doped samples were determined from the results obtained in the decomposition of dopant-free alloys, namely 1200 and 1100° C for T_7S_3 and T_3S_7 alloys (fabricated at 1400° C) and T_5S_5 alloy (1500° C), respectively.

Electrical conductivities of sintered bodies of dopant-free and doped alloys were measured to examine the role of the dopants in affecting phase separation in the TiO_2–SnO_2 system. Both surfaces of an as-fired body were polished and coated with silver by heating silver paste at 580° C. The temperature dependence of specific resistivity of a sample was evaluated using a digital LCR meter (YHP-4262A) by an a.c. two-probe method.

3. Results and discussion

3.1. Decomposition rate of TiO_2–SnO_2 alloys

3.1.1. Decomposition inside the coherent spinodal

In Fig. 2 XRD patterns are shown for T_5S_5 alloy annealed for 5 h at four different temperatures. Since spinodal decomposition in the present system produces compositional fluctuations along the [0 0 1] direction, XRD peaks with $(h\,k\,l)$ indices having $l \neq 0$ are split, while $(h\,k\,0)$ peaks exhibit no splitting. Splitting of the specified XRD peaks indicative of the coherent spinodal is clearly seen in the figure at the (2 1 1) peak in comparison with that of (2 2 0) for samples annealed below 1100° C. In annealing at higher temperatures or for longer times even at a low temperature, the coherency is lost and all the reflections are split.

Separation of phases by the spinodal mechanism proceeds by substitutional interdiffusion between Ti^{4+} and Sn^{4+}. Therefore, the rate of phase separation is determined by the occurrence and growth of composition fluctuations correlated with the diffusivity of mobile cations. That is, the decomposition rate should

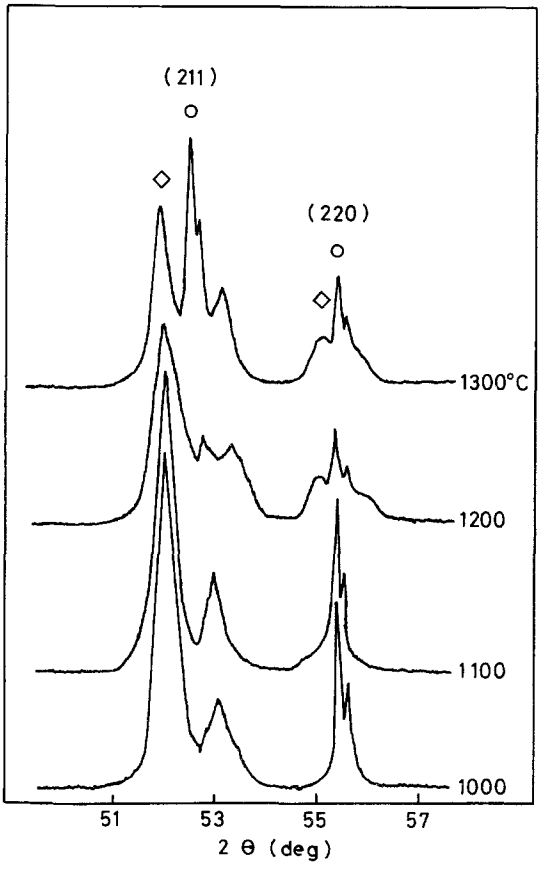

Figure 2 XRD patterns of equimolar T_5S_5 alloy annealed for 5 h at the temperatures shown. (○) Original alloy, (◇) tin-rich alloy.

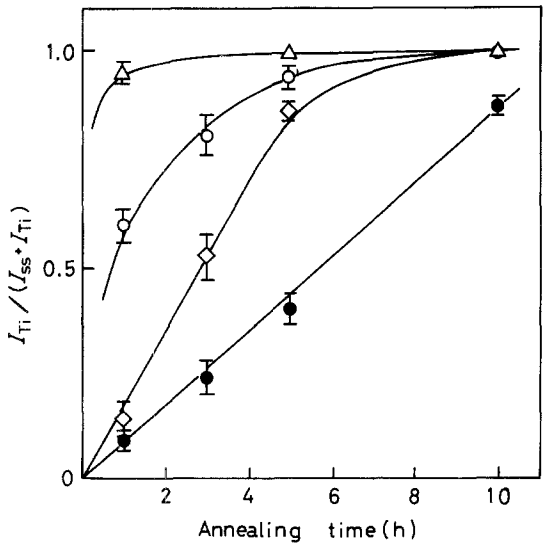

Figure 3 Temperature dependence of the phase separation of T_5S_5 alloy. (○) 1000° C, (△) 1100° C, (◇) 1200° C, (●) 1300° C.

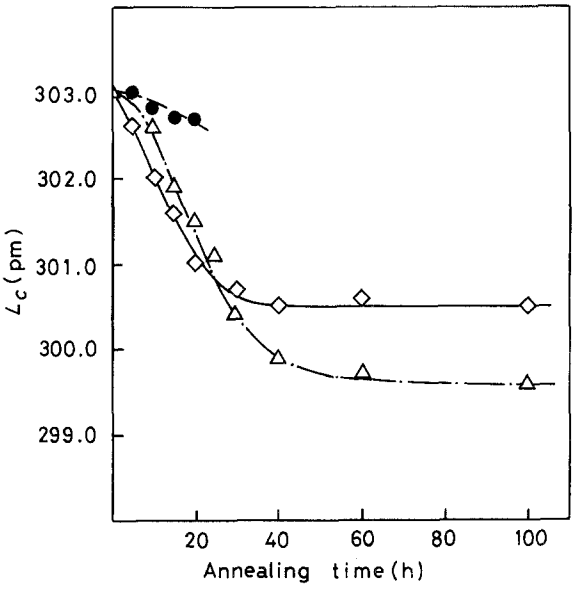

Figure 4 Lattice parameter change (L_c) of T_7S_3 alloy with annealing time. Annealing temperature (△) 1100° C, (◇) 1200° C, (●) 1300° C.

markedly depend on the annealing temperature. The temperature dependences are shown in Fig. 3 for an equimolar alloy annealed at 1000 to 1300° C for 1 to 10 h. The ordinate in this figure indicates the relation of the relative integrated intensity of the (2 1 1) peak of the original alloy (I_{ss} in Fig. 3), in which superimposed peaks could be separated by assuming a Gaussian distribution curve for an XRD profile, to that of titanium-rich alloy (I_{Ti}) produced by phase separation. It is evident that the decomposition of an equimolar alloy is most accelerated by annealing at 1100° C under the experimental conditions employed in this work. Hence large composition fluctuations combined with a relatively short diffusion path of ca. 20 to 30 nm, required in the early stage of spinodal decomposition [4], could result in a remarkably rapid phase separation. On the other hand, the retarded rate of phase separation observed in a sample annealed at 1300° C may be due to a very limited occurrence and growth of composition fluctuations, while maintaining fast ionic diffusion.

3.1.2. Decomposition outside the spinodal

In contrast with detailed investigations on the spinodal decomposition in the tetragonal oxide system, insufficient information is available on phase separation by the nucleation and growth mechanism [8]. T_7S_3 and T_3S_7 alloys were therefore annealed at 1100 to 1300° C for various times to elucidate the decomposition behaviour outside the coherent spinodal. In T_7S_3 alloy, the compositions of titanium-rich phases produced by annealing of the original alloy are, when representing the alloys as $Ti_xSn_{1-x}O_2$, $x_{1300} \approx 0.75$, $x_{1200} \approx 0.80$ and $x_{1100} \approx 0.84$ at each annealing temperature. As the phase separation proceeds, superimposed XRD peaks which are due to compositional similarity between the newly formed and original alloys are gradually shifted to final locations corresponding to those of a newly formed phase.

Changes in the lattice parameter L_c, calculated from the d values of several XRD peaks, are plotted against annealing times in Fig. 4. For samples annealed at 1300° C, few data are available in the figure because an estimated change in L_c of the sample must include much error, which might be attributed to very slight changes in the lattice parameters for the original and annealed alloys. Concerning the XRD results obtained in newly formed tin-rich phase whose XRD peaks are located at lower angles than those of the titanium-rich phase, nucleation seems to be substantially retarded at 1300° C. In annealing at lower temperatures, T_7S_3 alloy decomposes at a nearly constant rate followed by transitional decomposition to final equilibrium states, which are apparently achieved after 60 and 100 h annealing at 1200 and 1100° C, respectively. Comparing the decomposition rates of the samples annealed at different temperatures with an alternative basis of fractional change in lattice parameters, annealing at 1200° C caused more rapid phase separation in the early stage of the decomposition than that at 1100° C. In addition, diffraction profiles of the tin-rich phase produced at 1200° C became sharpened while appreciably broadened profiles appeared in samples annealed at 1100° C, indicating the formation of a large number of nuclei with inhibited growth.

For the phase separation of T_3S_7 alloy, XRD peaks of the newly formed titanium-rich phase were very small, particularly in the early stage of the decomposition. This might be not only caused by different atomic scattering factors for X-rays between titanium and tin atoms, but also by slower rates of decomposition compared with T_7S_3 alloy. The decomposition rate could alternatively be estimated from fractional changes in the lattice parameters of T_3S_7 alloy with annealing time. To calculate the parameter changes of the tin-rich phase, lattice parameters of the finally produced alloy, whose composition was determined from the phase diagram shown in Fig. 1, were used as reference parameters (L_a = 470.9 pm and L_c = 314.5 pm for $Ti_{0.2}Sn_{0.8}O_2$). The result is shown in Fig. 5 with a comparative presentation of the same change for T_7S_3 alloy. As is clearly seen from this figure, phase separation of T_3S_7 alloy is not yet

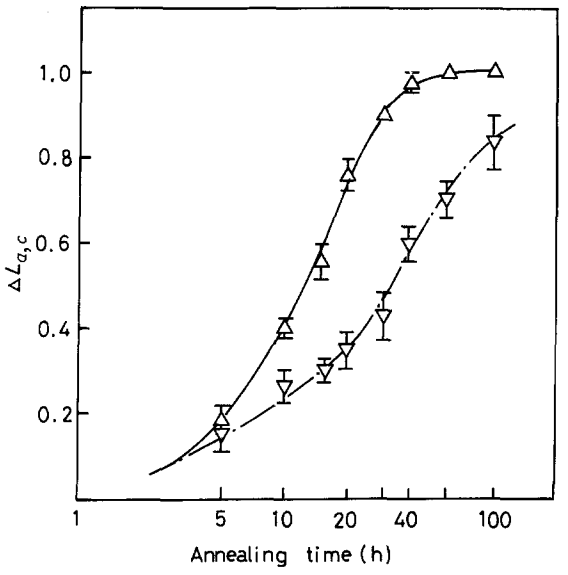

Figure 5 Fractional change in lattice parameters for (△) T_7S_3 and (▽) T_3S_7 alloys.

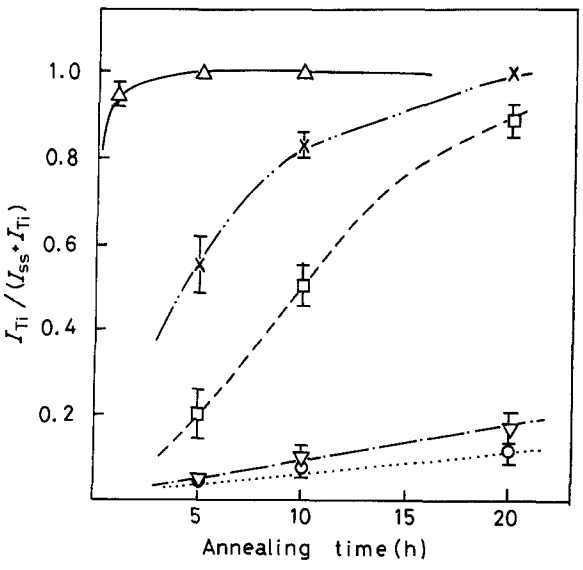

Figure 6 Decomposition curves of T_5S_5 alloy (△) dopant-free, and doped with (x) ZrO_2, (□) Ta_2O_5, (▽) WO_3 and (○) Sb_2O_3.

complete after annealing for 100 h, whereas ΔL can achieve a nearly constant value in a T_7S_3 sample annealed for 60 h, revealing the completion of phase separation.

Although some data on the diffusivity of titanium in TiO_2 crystals can be found in the literature [9, 10], the authors are not aware of any report on the self-diffusion of tin in SnO_2 and the separate diffusivity of titanium and tin in TiO_2–SnO_2 solid solutions. The result presented in Fig. 5, that is, a substantial difference in the rate of the phase separation after nucleation between T_7S_3 and T_3S_7 alloys, suggests that the ionic mobilities of diffusing species in the alloys, titanium and tin, might be greatly different. If the interdiffusion coefficient is strongly dependent on the concentration of a mobile species constituting a crystalline alloy, as in the case of interdiffusion in CoO–NiO [11], the rate of phase separation of the alloy, which is dominated by cation diffusion processes, will change as a function of alloy composition. Thus the retarded rate of decomposition observed in T_3S_7 alloy is probably attributed to the contribution of much slower diffusing tin in the present oxide alloys.

3.2. Effect of several dopants on phase separation

Little experimental work has been done on doping effects on phase separation in the present alloy system for decomposition inside and outside the spinodal. The doping effect of aluminium or tantalum on phase separation has been reported very concisely and interpreted using only a Frenkel or Shottky defect model [7, 8]. The authors therefore selected several dopants which had been determined from the preliminary examination of 14 dopants as decomposition-suppressing agents, and investigated the decomposition behaviour of several doped alloys (T_7S_3, T_5S_5, and T_3S_7) in detail.

Fig. 6 shows the rate of spinodal decomposition for doped T_5S_5 alloys which were annealed at 1100° C. The dopants used in the present experiments had a more or less suppressing effect on the decomposition. Among these effective dopants, the incorporation of tungsten or antimony atoms into the equimolar alloy remarkably decreased rapid phase separation by the spinodal mechanism. Additionally, the effects of the same dopants on the phase separation of T_7S_3 and T_3S_7 alloys are qualitatively presented in Fig. 7. Numerals of the ordinates and the abscissae in the figure indicate dopant concentration (mol %) and annealing time (h), respectively. An increase in the hatched region for each sample denotes an extension of decomposition. As is seen from Fig. 7, there is a little difference between the doping effects of the selected oxides on the suppression of phase separation of T_3S_7 alloy. In the case of T_7S_3 alloy, however, the dopants could be divided into two distinct groups according to their suppressing effect; dopants showing the effect with the addition of a relatively large amount (ZrO_2 and Ta_2O_5), and those acting as an excellent suppressor (WO_3 and Sb_2O_3). Doping with tungsten or antimony atoms resulted not only in a remarkable suppression of the decomposition of T_7S_3 alloy, but also in a much greater reduction of the decomposition rate than the other dopants for T_5S_5 and T_3S_7 alloys. Such a dependence of decomposition suppression on the doping species could not be merely rationalized with a defect model as described by Yuan and Virkar [8].

To obtain information about cation substitutions associated closely with electric structures of the doped alloys, the specific resistivities of several sintered bodies of dopant-free and doped samples were measured with an LCR meter during the process of cooling from 500° C. Temperature dependences of the specific resistivities are shown in Fig.8 for various alloys. In dopant-free alloys which indicate a semiconductive property with high values of the resistivity, the activation energies for the electric conduction, calculated from the linear part of the temperature dependence curve near 400 to 500° C, were found to be 1.0, 1.0, 0.82, and 0.45 eV for alloys having compositions of $x = 0.3$, 0.5, 0.7 and 0.9 in $Ti_xSn_{1-x}O_2$, respectively. It is well known that TiO_2 and SnO_2 are n-type semi-

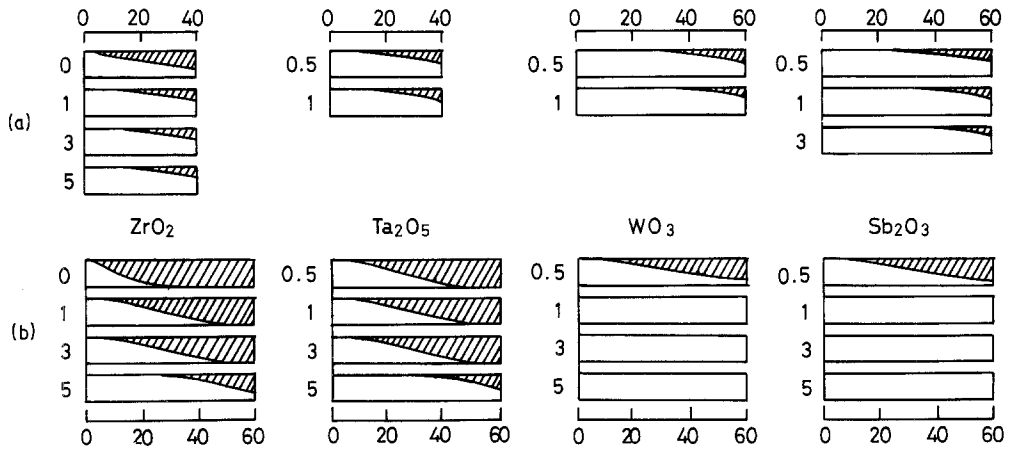

Figure 7 Schematic representation of doping effect on the phase separation of (a)T_3S_7 and (b)T_7S_3 alloys. Ordinates indicate dopant concentration (mol %) and abscissae the annealing times (h).

conductors induced by oxygen-deficient or metal-excess defect structures, in which donor levels are formed by the ionization of interstitial cations or by the emission of electrons trapped at oxygen vacancies. Assuming the band gaps of alloys of pure TiO_2 and SnO_2 to be 3.0 eV [12, 13] and 3.5 eV [14, 15], respectively, the changes gradually depending on alloy composition, a decrease in the activation energy with increasing titanium content might be caused by the formation of donor levels corresponding to the composition of the TiO_2–SnO_2 alloy.

In doped alloys having a much higher conductivity, except the ZrO_2-doped sample, the increasing conductivity may be ascribed to an increase in carrier concentration due to cation substitution with aliovalent atoms. Comparing the values and the temperature dependences of specific resistivity between tantalum-doped alloy and those containing the other two dopants, the tantalum-doped sample was apparently characterized by nearly the same electric properties independent of alloy composition. Conceivably a variation in the electric properties of doped alloys with doping species might be caused by selective substitution of the tin or titanium sublattice in the alloy. The selectivity of the cation substitution was then confirmed for the dopants by examining the separate solid solubilities of these dopants in TiO_2 or SnO_2. The results indicated that aliovalent atoms can be extensively soluble in TiO_2, whereas the incorporation of tantalum or tungsten into tin sites of SnO_2 seemed to be very limited. Furthermore, in a comparison of the solubilities of tantalum and tungsten in SnO_2, it was deduced that only a small amount of tantalum could be substituted in the tin sublattice, which was supported by the evidence obtained in the sintering of Nb_2O_5-containing SnO_2 [16]. On the other hand, a large amount of tungsten might be soluble in SnO_2, probably because of the partial formation of distorted rutile-type WO_2 with a lower oxidation state of W^{4+}. Thus doping with antimony or tungsten, which can be incorporated in the tin sublattice, resulted in a prolonged stabilization of the original alloys while a tantalum-doped sample in which most of the tantalum can be substituted in the titanium sublattice had little effect on the suppression of phase separation. Consequently, it was concluded that the phase separation involving spinodal decomposition in TiO_2–SnO_2 solid solutions can be extensively suppressed in doped samples in which foreign atoms capable of substitution in the tin sublattice can be easily incorporated.

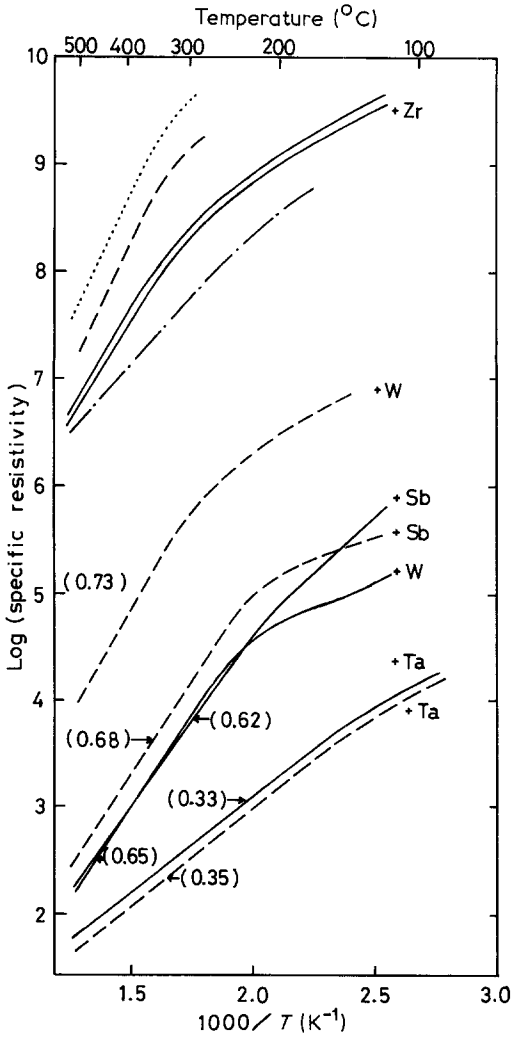

Figure 8 Temperature dependence of specific resistivity for dopant-free and doped alloys with comparative values of activation energy (eV). (···)T_3S_7, (– – –)T_5S_3, (——)T_7S_3, (–·–)T_9S_1.

References

1. M. PARK, T. E. MITCHELL and A. H. HEUER, *J. Amer. Ceram. Soc.* **58** (1975) 43.
2. J. W. CAHN, *Acta. Metall.* **9** (1961) 795.
3. *Idem, ibid.* **10** (1962) 179.
4. V. S. STUBICAN and A. H. SCHULTZ, *J. Amer. Ceram. Soc.* **51** (1968) 290.
5. A. H. SCHULTZ and V. S. STUBICAN, *Phil. Mag.* **18** (1968) 929.
6. M. W. PARK, T. E. MITCHELL and A. H. HEUER, *J. Mater. Sci.* **11** (1976) 1227.
7. A. V. VIRKAR and M. R. PLICHTA, *J. Amer. Ceram. Soc.* **66** (1983) 451.
8. T. C. YUAN and A. V. VIRKAR, *ibid.* **69** (1986) C-310.
9. T. S. LUNDY and W. A. COGHLAN, *J. Phys. (Paris) Colloq.* **1973** (1973) 299.
10. J. R. AKSE and H. B. WHITEHURST, *J. Phys. Chem. Solids* **39** (1978) 457.
11. W. K. CHEN and N. L. PETERSON, *ibid.* **34** (1973) 1093.
12. D. C. CRONEMEYER, *Phys. Rev.* **87** (1952) 876.
13. P. MOCH, M. BALKANSKI and P. AIGRAIN, *C. R. Acad. Sci.* **251** (1960) 1373.
14. K. J. BUTTON, D. G. FONSTAD and W. DREYBRADT, *Phys. Rev.* **4B** (1971) 4539.
15. J. ROBERTSON, *J. Phys. C.* **12** (1979) 4767.
16. J. TAKAHASHI, I. YAMAI and H. SAITO, *Yogyo-Kyokai-Shi* **83** (1975) 54.

Received 12 May
and accepted 22 July 1987